HHS Public Access

Author manuscript

Nat Microbiol. Author manuscript; available in PMC 2018 July 20.

Published in final edited form as:

Nat Microbiol. ; 1: 16011. doi:10.1038/nmicrobiol.2016.11.

Dynamics of the human and viral m^{6}A RNA methylomes during HIV-1 infection of T cells

Gianluigi Lichinchi[1,2], **Shang Gao**[1], **Yogesh Saletore**[3], **Gwendolyn Michelle Gonzalez**[4], **Vikas Bansal**[1], **Yinsheng Wang**[4], **Christopher Mason**[3], and **Tariq M. Rana**[1,2,*]

[1]Department of Pediatrics, University of California, San Diego School of Medicine, La Jolla, California 92093

[2]Program for RNA Biology and Graduate School of Biomedical Sciences, Sanford Burnham Prebys Medical Discovery Institute, 10901 North Torrey Pines Road, La Jolla, California 92037

[3]Department of Physiology and Biophysics and the Institute for Computational Biomedicine, Weill Cornell Medical College of Cornell University, 1305 York Ave., New York, New York 10021

[4]Environmental Toxicology Graduate Program and Department of Chemistry, University of California, Riverside, California 92521.

Abstract

N^6-methyladenosine (m^{6}A) is the most prevalent internal modification of eukaryotic mRNA. Very little is known of the function of m^{6}A in the immune system or its role in host–pathogen interactions. Here we investigated the topology, dynamics, and bidirectional influences of the viral–host RNA methylomes during HIV-1 infection of human CD4 T cells. We show that viral infection triggers a massive increase in m^{6}A in both host and viral mRNAs. In HIV-1 mRNA, we identified 14 methylation peaks in coding and noncoding regions, splicing junctions, and splicing regulatory sequences. We also identified a set of 56 human gene transcripts that were uniquely methylated in HIV-1-infected T cells and were enriched for functions in viral gene expression. The functional relevance of m^{6}A for viral replication was demonstrated by silencing of the m^{6}A writer or the eraser enzymes, which decreased or increased HIV-1 replication, respectively. Furthermore, methylation of two conserved adenosines in the stem loop II region of HIV-1 Rev Response Element (RRE) RNA enhanced binding of HIV-1 Rev protein to the RRE in vivo and influenced nuclear export of RNA. Our results identify a new mechanism for the control of HIV-1 replication and its interaction with the host immune system.

*Correspondence and request for materials should be addressed to T.M.R. (trana@ucsd.edu).

Author Contributions

G.L. designed and performed experiments, analyzed data, wrote the paper; S.G. performed experiments and analyzed data; Y.S. performed experiments and analyzed data; G. M. G. performed experiments and analyzed data; V.B. analyzed data; Y.W. analyzed data; C.M. analyzed data; T.M.R. concept, design, data analysis, manuscript writing, and financial support.

Additional information

Supplementary information is available online. Reprints and permissions information is available online at www.nature.com/reprints. Correspondence and requests for materials should be addressed to T.M.R.

Competing interests

The authors declare no competing financial interests.

INTRODUCTION

RNA plays numerous vital roles in cellular processes ranging from the transfer of genetic information from DNA to protein to the epigenetic modulation of gene transcription[1]. Similarly to proteins and DNA, RNA undergoes chemical modifications that can influence its metabolism, function, and localization. More than 100 diverse chemical groups are known to modify RNA at one or more of its four nucleotides (A, G, C, and U). Ribosomal and tRNAs sequences incorporate most of the diverse chemical modifications. Other than the 5′-cap structure, mRNAs and IncRNAs contain N6-methyladenosine (m6A) and 5-methyl cytosine (m5C)[2,3]. Methylation of adenosine at the N6 position (m^6A), which was first reported ~40 years ago[4-7], is the most prevalent internal modification of eukaryotic mRNA and contributes to its generation, localization, and function[8-10]. Although our understanding of the importance of m^6A to physiological and pathological processes is increasing rapidly[11-13], little is known of the function of m^6A in the mammalian immune system or its role in host–pathogen interactions.

Adenosine methylation is catalyzed by a “writer”, which is a large 1 MDa RNA methyltransferase complex (MTase) composed of two catalytic subunits (METTL3 and METTL14), a splicing factor (WTAP), a novel protein (KIAA1429), and other subunits not yet identified[10,14-16]. Conversely, methyl groups are removed by two “erasers” RNA demethylases, FTO and AlkBH5[12,13]. The development of techniques to selectively immunoprecipitate m^6A and sequence the associated RNA (MeRIP-seq) has been pivotal to our understanding of the topology and prevalence of m^6A in various eukaryotic transcriptomes[8,9]. Also, the mRNA regions most highly enriched in m^6A are transcription start sites, stop codons, and 3′UTRs[8-10], raising many hypotheses about their roles. Methylation of RNA adenosines is a dynamic process and the exact sites and frequency of modification may vary in cells exposed to non-physiological conditions such as stress, inflammation, and infection.

Although the precise molecular functions of m^6A and its dynamic regulation are not yet fully understood, it has been postulated to play several important roles in RNA metabolism, including translation, stability, splicing, transport, and localization[17,18]. For example, the enrichment of m^6A in regions of the 3′UTR plays a role in RNA stability through specific recognition of m^6A sites by RNA-binding proteins involved in mRNA decay pathways[19-21]. m^6A modification is involved in triggering RNA structural switches to affect RNA-protein interactions[22] as well as directing translational control of heat shock responses[23]. Additionally, nuclear export of mRNA is promoted by the increased abundance of m^6A resulting from AlkBH5 depletion[13]. m^6A is enriched in exonic regions flanking splicing sites[24]. Increased m^6A resulting from FTO knockout favours the binding of splicing factor SRSF2 to mRNA splicing sites and in turn promotes inclusion of target exons[24]. Circadian gene expression is delayed upon METTL3 depletion[25], and pluripotency of embryonic stem cells is affected by modulation of METTL3[26,27] and METTL14[28] expression. Taken together, these findings substantiate RNA methylation as a new epitranscriptomic mechanism for the regulation of gene expression.

The internal m^{6}A modification is also present in viral RNA. This was first identified in Rous sarcoma virus[29], influenza virus[30], and SV40 virus[31] several decades ago, but the function and relevance of this modification to viral replication remain unclear. Similarly, whether and how viral infections alter the dynamics of the host or viral RNA methylomes remain fundamental and unanswered questions. Notably, m^{6}A has not yet been identified in HIV-1 RNA. In this study, we report the presence of this modification in HIV-1 RNA and examined the topology, functions, and molecular features of m^{6}A in both HIV-1 and host RNA during infection of human CD4+ T cells.

RESULTS

RNA methylation in T cells is enhanced by HIV-1 infection and modulates viral replication

To investigate whether HIV-1 RNA is m^{6}A modified during the course of viral infection, we examined the MT4 human CD4+ T cell line at 3 days post-infection with the HIV-1 LAI clone, the time period when virus is in the active replication phase. The abundance of m^{6}A was analysed by anti-m6A immunoblotting (Fig 1a) and quantified by LC-MS/MS according to published methods [32]. Poly(A) RNA from LAI-infected cells showed significantly higher level of m^{6}A (~30% increase) compared with control uninfected cells (Fig. 1b). An increase in methylation was observed in all RNA sizes (Fig. 1a, middle panel), suggesting a widespread effect on cellular mRNA species. These results were also confirmed by m^{6}A immunoblot analysis of poly(A)-enriched RNA where the contribution of ribosomal RNA was removed (Supplementary Information Fig. 1). Total RNA from HIV-1-infected cells showed a high molecular weight band with an intense m^{6}A signal, which was subsequently identified as HIV-1 genomic RNA by northern blot analysis (Fig. 1a, middle and right panels). These results demonstrate that HIV-1 infection of T cells promotes methylation of both viral and host RNA.

We next determined whether modulation of m^{6}A abundance might alter the HIV-1 replication rate. MT4 cells were transduced with shRNAs targeting METTL3, METTL14, or AlkBH5, and knockdown efficiency was assessed by western blot and RT-qPCR analysis (Supplementary Information Fig. 2). We chose to deplete AlkBH5 for RNA demethylase function due to its high expression in T cells. Transduced cells were then infected with HIV-1 LAI and 3 days later, viral replication was monitored by RT-qPCR analysis of gp120 mRNA levels and p24 immunoblotting of total cell extracts (Fig. 1c, d). Depletion of METTL3 or METTL14 alone significantly decreased viral replication compared with cells expressing nontargeting control (NTC) shRNA, and an additive effect was observed when both MTases were simultaneously knocked down. Conversely, AlkBH5 silencing caused a striking increase in viral replication (Fig. 1c, d). Taken together, these results demonstrate that modulation of METTL3, METTL14, and AlkBH5 expression directly affects HIV-1 replication.

Topology of RNA methylome during HIV-1 infection

We next examined the topology of the m^{6}A RNA methylome during HIV-1 infection by MeRIP-seq experiments. Poly(A)-enriched RNA from uninfected and HIV-1-infected MT4 cells was fragmented into 60–200 nucleotides and immunoprecipitated using an m^{6}A-

specific antibody (see methods), and the associated RNA was then sequenced. Reads were mapped onto the HIV-1 and human genomes to identify regions enriched in m^6A. We found ~ 49% of input RNA-seq reads and ~ 42% of MeRIP-seq reads mapped to the HIV genome, respectively (Supplementary Information Table 1). We identified 14 distinct methylation peaks located in coding and noncoding regions, splicing junctions (D1), and splicing regulatory sequences (Fig. 2a; Table 1), with each peaks suggesting potential specific functional roles for each methylation peak. Peak 1 encompasses the primary binding site sequence, dimerization sequence, encapsidation sequence (ψ), D1 splicing site, and *gag* gene start site. Peak 2 is within the *gag* coding sequence. Peak 3 overlaps the *gag* gene stop codon and the *pol* gene start codon. Peaks 4-7 are within the *pol* coding sequence. Peak 8 is within the *vif* coding sequence and also overlaps with the exonic splicing enhancer for *vpr* (ESEVpr). Peak 9 overlaps with the exonic splicing silencer 2p (ESS2p) the exonic splicing silencer 2 (ESS2) and *vpr* coding sequence. Peak 10 lies within the *env* coding sequence. Peak 11 overlaps with the RRE region. Peak 12 is within the *env* and *rev* coding sequences, and overlaps the *tat* gene stop codon and the exonic splicing enhancer 3a (ESS3a). Peak 13 lies upstream of the *env* gene stop codon and the *nef* gene start codon. Peak 14 is within the *nef* coding sequence. These findings identify the topology of the m^6A landscape in HIV-1 RNA and indicate widespread methylation throughout the genome.

Next, we performed MeRIP-seq experiments to determine the dynamics of RNA methylation in the host cells after HIV-1 infection, and identified a set of 56 gene transcripts that were specifically methylated upon viral infection (Supplementary information Table 2 and Supplementary information Fig 3). We performed gene ontology (GO) analysis of the 56 genes and found that the most represented category was “viral gene expression”, suggesting that methylation of many of the transcripts is functionally important for viral infection (the top 10 most enriched categories are shown in Supplementary Information Fig. 3a). In fact, of the 56 genes, 19 have a known association with HIV replication, and in some cases, the protein products directly interact with viral components. Remarkably, the majority of these genes encode proteins with proviral functions. Depletion or inhibition of MOGS, PSIP1 (LEDGF), HNRNPK, TRAF2, TUBA1B, CCT2, PABPC3, CBFB and ETS2 have been reported to negatively affect different viral replication steps (see Supplementary information Table 2 and references therein); expression of GTF2I, MYL12A, and UBA52 is induced by the infection process or by viral proteins; HLA-DPA2, EIF3M, DUT, MBD2, and RPS5 proteins have been shown to interact with viral proteins; and HSPA1A and SRSF5 overexpression is known to promote viral replication.

The exact mechanism by which m^6A regulates the stability, splicing, and translation of RNA transcripts remains unknown. To gain insight, we compared the distribution of m^6A peaks in the 56 HIV-1-specific methylated RNAs versus the total infected cellular transcriptome and found some striking differences (Fig. 2b). Specifically, the percentage of total m^6A peaks mapping to the human genome located in the 5′UTR, CDS, 3′UTR, and intronic regions was 17.5%, 66.0%, 14.4%, and 2.1% for the 56 HIV-specific m^6A peaks, respectively, compared with 13.4%, 41.0%, 31.6%, and 14.0% for the same regions in the total cellular transcriptome of infected cells (Fig. 2b). Thus, for the HIV-1 specific methylated genes, m^6A is more abundant in the 5′UTR and CDS and less abundant in the 3′UTR and intronic regions of HIV-1 RNA compared with total cellular mRNA. These findings suggest that

m^{6}A modification may have more prominent functions in RNA splicing and translation than in RNA stabilisation. Additionally, m^{6}A appears to be more prevalent on mature than immature mRNAs, as indicated by the large reduction of m^{6}A peaks in the intronic region of HIV-1 RNA versus total cellular mRNA.

RNA methylation is a dynamic process controlled by the catalytic activities of the m^{6}A writer (MTases) and eraser (demethylases) enzymes. Because the enzymes have preferred target sequences[8,9,13,18,19], we performed consensus sequence motif analysis within m^{6}A peaks to determine the preferred motifs in HIV and cellular RNA, and determined whether the preferential motif usage in the host cells was altered by HIV-1 infection. In uninfected T cells, the frequency of MGACK (A/C-GAC-G/U), RRACH (G/A-G/A-AC-A/C/U), and UGAC motifs within m^{6}A peaks was ~37%, 33%, and 30%, respectively (Fig. 2c). After HIV-1 infection, enrichment of m^{6}A in motif MGACK was increased (37% to 42%), indicating a large change in motif preference during viral infection. In HIV-1 RNA, UGAC and MGACK were equally preferred (~37%), but UGAC usage was ~7% higher than in the cellular transcripts. Although the mechanisms by which viral infection drives a change in the preferred host m^{6}A motif are not clear, several plausible possibilities exist. For example, the assembly and catalytic rate of the methylation complex may be changed by viral infection such that MGACK becomes the preferred substrate. Conversely, infection-driven changes in demethylase activities may decrease recognition of methylated MGACK but not of the other sequence motifs. Or, the accessibility of these motifs is altered in this context, either by sequestering or secondary structure. Future characterization of methylation complexes in HIV-1-infected cells will undoubtedly enhance our understanding of the dynamics of mammalian and viral RNA methylation during host–virus interactions.

m^{6}A methylation modulates the interaction between Rev protein and RRE RNA

In considering the mechanism by which m^{6}A might alter RNA function to promote HIV-1 replication, we hypothesized that m^{6}A might alter the secondary or tertiary structures of RNA and subsequently its ability to interact with proteins. To test this, we examined binding of viral Rev protein to RRE RNA. RRE is a structurally and functionally well-characterized RNA element within the HIV-1 *env* gene. After translation, Rev proteins are imported back into the nucleus where they assemble at the RRE to form active nuclear export complexes that facilitate transit of viral transcripts into the cytoplasm[33-35]. This is an essential step in viral replication. Intriguingly, we found that peak 11 of the HIV-1 methylation sites (Fig. 2a) spanned the stem IIB region of RRE RNA, which contains the high-affinity binding site for Rev (Fig. 3a). The stem loop secondary structure of RRE is critical for Rev protein binding and its function in nuclear export of HIV-1 RNA[33-35]. The solution structure of a Rev peptide bound to stem loop IIB showed that Rev binds in the major groove of the RRE in a distinctive binding pocket formed by two purine-purine base pairs[36]. Therefore, we reasoned that methylation of A7877 and A7883 in stem loop IIB (Fig. 3a) might affect the RRE affinity for Rev and thus alter the function of the RNA-protein complex.

To test this possibility, we first determined whether METTL3/METTL14 or AlkBH5 knockdown in MT4 cells modulated the methylation status of RRE RNA and its interactions with Rev. MeRIP experiments coupled with RT-qPCR specific for the RRE sequence first

confirmed that the two MTases and the demethylase are indeed able to methylate and demethylate RRE, respectively (Supplementary Information Fig. 4a). Silencing of METTL3/14 decreased the amount of RRE RNA by Me-RIP while knock down of AlkBH5 enhanced RRE RNA isolated by Me-RIP (Supplementary Information Fig 4a). To determine whether changes in RRE methylation affect its affinity for Rev, we performed experiments in 293T cells transiently expressing the HIV-1 construct pLAI2. Rev–RRE interactions were detected by immunoprecipitation of Rev followed by qPCR to quantify bound RRE RNA. We found that Rev–RRE binding was significantly reduced by silencing of METTL3/METTL14 and, conversely, significantly increased by AlkBH5 knockdown (Fig. 3b). These results demonstrate that methylation of RRE RNA enhanced the formation of Rev–RRE complexes in vivo. Analysis of the REV immunoprecipitates indicated that these effects were not due to differences in the efficiency of Rev immunoprecipitation between cells expressing the various shRNAs (Supplementary Information Fig. 4c).

Because these experiments were performed with 293T cells expressing full-length HIV-1, it is possible that other viral proteins may have influenced Rev–RRE binding. To address this concern, we performed the same experiments with cells expressing FLAG-Rev and the 66-nucleotide minimal RRE stem loop region (Fig. 3a). Consistent with the results in cells expressing the full-length HIV-1 RRE, we found that Rev binding to the minimal RRE sequence was significantly decreased by METTL3/METTL14 knockdown and increased by AlkBH5 knockdown (Supplementary Information Fig. 4b and c). These data strongly suggest that modulation of A7877 and A7883 methylation in the RRE stem loop IIB region affects its binding to Rev protein.

Rev-RRE interactions and their function in nuclear export of viral RNAs are required events in HIV-1 replication cycle. We asked if the changes in the binding ability of Rev to RRE due to the alteration of RNA methylation could affect the function of viral RNA export. We depleted METTL3/METTL14 or AlkBH5 in 293 cells by corresponding shRNAs followed by infections with HIV-1 LAI virus. Next, we prepared cytoplasmic and nuclear fractions from these cells and quantified RRE RNA distribution in the cytoplasm and nucleus. Hypo-methylation of RRE caused by METTL3/METTL14 knockdown significantly decreased viral RNA nuclear export, consistent with the observed reduction in replication rates. On the contrary, hypermethylation of RRE RNAs by AlkBH5 silencing was able to enhance nuclear export and viral replication (Supplementary Information Fig 4d; and Fig 1c).

In order to define which adenosine in the RRE hairpin structure is methylated in vivo, we performed primer extension experiments using AMV RT and *Tth* DNA polymerase [37]. A7877 and A7883 modifications were analysed by sequence-specific complementary ssDNA probes and enzymatic extensions. In contrast with AMV RT, *Tth* pol enzyme is sensitive to m^6A RNA modification resulting in markedly reduced ability to extend the DNA oligo. As shown in Fig 3c, *Tth* pol failed to extend the probes for both A7877 and A7883 sites, indicating that these A residues are methylated in vivo. In control experiments using ribosomal RNA, *Tth* pol extended oliogs for A4189 (unmethylated site) and did not extend to A4190 (methylated site), which are consistent with previously reported results [37]. Altogether, these results show that the both A in the RRE hairpin are methylated in vivo. m^6A methylation of RRE may influence Rev binding by at least two mechanisms; direct

interaction of the methyl group with specific Rev residues and/or by inducing changes in RRE folding and thus the secondary structure required for Rev recognition. Further experiments will be necessary to clarify the mechanisms involved.

HIV-1 replication and RNA nuclear export are perturbed by methylation of A7883 in the RRE bulge region

To determine whether m^6A methylation in RRE RNA might confer an evolutionary advantage for HIV-1, we analysed the mutation frequency of A7877 and A7883 in 2,501 HIV-1 sequences isolated from infected humans. For this, we downloaded aligned FASTA sequences from the HIV database and processed the alignments using a custom Python program. At each position in the reference HIV-1 HXB2 genome, we calculated the frequency of mutations (single nucleotide substitutions and insertions/deletions) using the alignment matrix for the 2,501 sequences (Supplementary Information Fig. 5). We found that the mutation frequencies at positions A7877 and A7883 were 5.44% and 0.28%, respectively, which are much lower than the mutation frequencies of other adenosine residues in the HIV-1 sequence or of the adenosines in the stem loop IIB region of RRE (11.16 ± 0.30% s.e.m. and 8.99 ± 6.80% s.e.m, respectively; Supplementary Information Fig. 5). This analysis suggests that A7877 and A7883 in the RRE are conserved and likely to confer survival benefit. Interestingly, A7883 is located immediately above the high-affinity Rev-binding internal bubble structure of RRE stem loop IIB (Fig. 3a)[38,39]. Collectively, these results demonstrate a significant role for A7877 and A7883 in Rev–RRE binding and function.

In order to further validate the role of specific methylation at position A7877 and A7883 in HIV-1 replication, we generated LAI mutant constructs in the RRE region (Fig 3a): U7871C + A7877G (Mut1), A7883G (Mut2) and the combination of both (Mut3). The mutant constructs were assessed for viral replication by transfecting 293T cells with WT or mutant pLAI2 plasmids (Fig. 4a). Mut1, which is designed to affect methylation at position A7877, did not show relevant differences in terms of viral expression in NTC, METTL3/METTL14 or AlkBH5 knock-down conditions compared to WT virus. On the other hand, Mut2 and Mut3, which are mutated at the bulge region of RRE A7883, show dramatic decrease in viral replication (~10% compared to WT) and this effect is not modulated by METTL3/METTL14 or AlkBH5 Knock-down, suggesting that mutation at A7883 is not only responsible in severely attenuating viral fitness but also a functionally critical nucleotide modified by the cellular RNA methylation machineries. Furthermore, we analyzed the nuclear export efficiency of the mutant constructs and compared with the WT virus (Fig. 4b). Mutations at the A7877 region (Mut1) did not perturb the nuclear export efficiencies of viral transcripts, while mutations at A7883 in the bulge region (Mut2 and Mut3) drastically affected nuclear export of viral RNA (Fig 4b). Taken together, these results demonstrate that methylation at A7883 is critical for Rev binding, enhanced nuclear export, and viral replication.

DISCUSSION

Based on these studies, we propose a model for m^{6}A methylation of RRE RNA and its effects on HIV-1 replication (Fig. 5). Silencing of METTL3/METTL14 or AlkBH5 induces m^{6}A hypomethylation or hypermethylation of HIV-1 RRE sites at positions A7877 and A7883, respectively. Rev protein preferentially interacts with methylated RRE. Therefore, AlkBH5 silencing increases RRE RNA methylation and thus promotes Rev binding, increases nuclear export of viral RNA, and subsequently, viral replication. In contrast, METTL3/14 silencing reduces methylation of RRE RNA and subsequent Rev recruitment onto the RRE, thereby reducing export of viral RNA and suppressing replication. Our results presenting the significance of A7883 in Rev-RRE interactions is further supported by in vitro Rev-RRE binding and NMR studies. In vitro experiments determined that efficient Rev binding required A7883 in the RRE structure [40]. NMR structural studies have shown that A7883 is flipped out from the stem region of RRE and directly interacts with W45 of Rev through van der Waals contacts[36]. Notably, mutation of W45 inactivates Rev[41]. Recent studies further highlight the significance of m^{6}A RNA modification in regulating the dynamics of RNA structure and RNA-protein interactions involved in biological mechanisms [22,42-44].

In summary, this work highlights the significance of RNA methylation in the context of HIV-1 infection in human T cells. The demonstration that viral infection significantly increases m^{6}A abundance in both viral and host cell RNA provides an impetus to further investigate the role played by RNA methylation in HIV-1 biology and in the mammalian response to viral infection. The topology of m^{6}A methylation in HIV-1 RNAs shows unique features compared to cellular mRNAs. m^{6}A is abundant across the full-length viral genome and is present in regulatory regions, coding sequences, and structural regions, suggesting that multiple aspects of viral RNA biology may be regulated by m^{6}A, possibly through distinct mechanisms. We found that the RNA methylation status positively correlates with viral replication, revealing a previously unknown layer of regulation of HIV-1 replication. Precise loci of methylation can be further investigated by single-molecule technologies, which are just emerging [45] and also enabled fully-phased epitranscriptomic characterization of viruses, thus revealing the co-occurrence of these dynamic m^{6}A sites. Finally, our finding that Rev–RRE binding is regulated by MTases and demethylases suggests that the pathways could be exploited pharmacologically to disrupt Rev function. Overall, these results identify a new mechanism for the control of HIV-1 replication and its interaction with the host immune system. These findings also suggest that other RNA viruses may similarly utilize the m^{6}A RNA modification as a mechanism to regulate viral and host RNA metabolism and gene regulation.

METHODS

Additional Methods are available on Online Content

HIV-1 virus production and MT4 infection.—HIV-1 LAI virus was produced by transfection of 293T cells with the proviral pLAI2 plasmid (NIH AIDS Reagent Program) at 3 μg/10^6 cells using Lipofectamine 2000 (Invitrogen), according to the manufacturer's instructions. After 4 h incubation, the medium was replaced with DMEM supplemented with

10% foetal bovine serum (FBS). Two days after transfection, the virus-containing supernatant was collected and filtered. The human T cell line MT4 was then infected with HIV-1 LAI virus (10^6 cpm of RT activity/10^6 cells), and 12 h later, the cells were centrifuged to remove the virus, washed with PBS, and resuspended in RPMI/10% FBS for further analysis. MT4 and 293T cells were obtained from ATCC and were tested for the absence of mycoplasma.

m^{6}A immunoblot analysis.—Total RNA was extracted from uninfected or HIV-1-infected MT4 cells (at 3 days post-infection) with TRIzol reagent (Invitrogen). Aliquots of 5 μg total RNA were separated on 1% agarose/0.4% formaldehyde gels in 20 mM HEPES and 1.5 mM EDTA, pH 7.8. RNA was stained with ethidium bromide and transferred overnight to nitrocellulose membranes in 10X SSC buffer (1.5 M NaCl, 150 mM sodium citrate). RNA was UV-crosslinked to membrane and blocked in 5% milk PBS Tween 0.1%. Rabbit polyclonal anti m6A antibody was used at 1:1000 dilution in PBS Tween 0.1% with incubation at room temperature for 1 hour. Subsequent steps for m^{6}A immunoblotting were performed according to previously reported protocols[8]. For m^{6}A dot blotting, poly(A) RNA was purified with an mRNA Direct Kit (Ambion) and the remaining steps were as described above. Densitometric quantification of the m^{6}A signal intensity was performed using ImageJ software (NIH).

m6A-modified RNA immunoprecipitation sequencing (MeRIP-seq) and analysis.—The quality of the RNA samples was assessed using an Agilent Bioanalyzer RNA 6000 Nano kit to ensure all RNA integrity numbers were >9.0. For poly(A) RNA purification, Dynabeads Oligo(dT)$_{25}$ (#61005, Life Technologies) were incubated with an aliquot of 75 μg RNA, washed, and subjected to a second incubation with the same RNA sample, according to the manufacturer's instructions. RNA was obtained by ethanol precipitation overnight, fragmented using Ambion® RNA Fragmentation Reagents (#AM8740, Life Technologies), and then repurified by ethanol precipitation overnight. An aliquot of fragmented RNA was retained as a control for RNA sequencing.

For MeRIP, fragmented RNA was denatured for 5 min at 75°C, cooled on ice for 2–3 min, and incubated with the anti-m^{6}A-coupled beads in 300 μl of 140 mM IP Buffer for 2 h at 4°C. Unbound RNA was removed by centrifugation, and beads were washed three times with 140 mM IP buffer and then incubated in elution buffer (5 mM Tris HCl, pH 7.5, 1 mM EDTA, 0.05% SDS, and proteinase K) for 1.5 h at 50°C. The eluted RNA was extracted with phenol/chloroform and precipitated with ethanol. An aliquot of RNA was retained as a control for round 1 MeRIP RNA, and the remainder was subjected to a second round of MeRIP, as described above. Libraries for sequencing (input RNA-Seq and MeRIP-Seq) were prepared using Illumina TruSeq Stranded mRNA kits, entering the protocol at the Elute-Prime-Fragment step, with the modification that samples were heated to 80 °C for 2 mins to only prime but not further fragment. Samples were sequenced on a HiSeq 2000 across 2 lanes with single read 50. RNA-seq data were aligned to a combined hg19 (chr 1-22, X, Y) and HIV-1 (https://aidsreagent.org/, pLAI2) genome FASTA using the STAR aligner[46] keeping only uniquely mapping reads. Peaks were called with MeRIPPeR[8], using Fisher's Exact Test on 25 bp genome-based windows to test for statistically significant enrichment in

the IP relative to the control input RNA, with Benjamini-Hochberg p-value adjustment and a p-value cutoff of 0.05. Windows were merged into peaks and peaks smaller than 100 bp were filtered out. Differentially methylated peaks were called by splitting the union of all peaks into 100 bp windows in 25 bp steps. MeRIP-seq and RNA-seq counts were tabulated using bedtools[47]) and input into edgeR[48] to identify windows with significant changes in methylation. Read counts mapping to genes were obtained using HTSeq (HTSeq cite), gene features using R-Make count (http://physiology.med.cornell.edu/faculty/mason/lab/r-make/usage.html), and all other features using BedTools. RNA-Seq data are publicly available at GEO GSE74016.

Gene ontology (GO) analysis of the uniquely methylated transcripts identified during HIV-1 infection was performed using AmiGO software. The top 10 categories are shown.

Rev–RRE interaction experiments.—For the Rev-RRE interaction experiments, we transfected 3 μg pLAI2 plasmid per 10^6 293T cells. After 4 h, the medium was replaced with fresh DMEM/10% FBS and incubated for a further 44 h time period. Cells were then lysed in IP lysis buffer (Pierce) and Rev protein was immunoprecipitated by incubation overnight at 4 °C with anti-Rev antibody [49] (NIH AIDS Reagent Program) (5 μg/10 × 10^6 cell equivalents) and 50 μl protein A/G magnetic beads (Pierce). For overexpression of Rev protein, the Rev coding sequence was amplified from cDNA isolated from HIV-1-infected MT4 cells and cloned into pFLAG-CMV-2 (Sigma) using EcoRI and SalI restriction sites. A minimal RRE corresponding to a 66 nucleotide region (GCA CTA TGG GCG CAC GGT CAA TGA CGC TGA CGG TAC AGG CCA GAC AAT TAT TGT CTG GTA TAG TGC) was PCR amplified and cloned into pcDNA3 (pcDNA3_minRRE) using HindIII and EcoRI restriction sites. The FLAG-Rev construct (1.5 μg) was co-transfected with pLAI2 (1.5 μg) or pcDNA3_minRRE (1.5 μg) into 10^6 293T cells with Lipofectamine 2000. After 4 h, the medium was replaced with fresh DMEM/10% FBS and incubated for a further 44 h. Cells were then lysed in IP lysis buffer (Pierce) and Rev protein was immunoprecipitated by incubation for 2 h at room temperature with anti-FLAG antibody (2 μg/3 × 10^6 cell equivalents) and 10 μl protein A/G magnetic beads (Pierce). IPs with mouse IgG (Santa Cruz Biotechnology) were performed in parallel as negative controls. In all the experiments, the beads were washed three times with IP lysis buffer and divided into equal volumes. One aliquot was extracted with TRIzol for RRE RNA quantification by qPCR, with normalization to β-actin RNA. The second aliquot was subjected to western blotting to assess anti-FLAG IP efficiency.

MeRIP-qPCR analysis of RRE methylation.—MT4 cells (5 × 10^6) were transduced with lentiviruses encoding METTL3, METTL14, or AlkBH5 shRNA as described above. After 3 days, cells were infected with LAI virus and RNA was extracted 48 h later. Aliquots of 40 μg total RNA were poly(A) enriched using mRNA direct isolation kit (Ambion) and enriched fractions were fragmented into 60–200 nucleotides with RNA fragmentation reagents (Life Technologies #AM8740). Fragmented RNA was incubated with 3 μg anti-m^6A and 15 μl protein A/G magnetic beads for 2 h at room temperature in MeRIP buffer (10 mM Tris HCl, 150 mM NaCl, 0.1% NP-40, pH 7.4). IPs with rabbit normal IgG (10500C, Invitrogen) were performed in parallel and served as input controls. Beads were washed

three times with MeRIP buffer, and m^6A-containing RNAs were eluted by incubation with 20 mM m^6A for 20 min at room temperature. Eluted RNA fractions were precipitated using the sodium acetate/ethanol precipitation method, and cDNA synthesis and qPCR analysis were performed as described above.

AMV Reverse Transcriptase and *Tth* DNA polymerase primer extension analyses for probing site-specific m6A modification.—These experiments were performed as previously described [37] with the following modifications. ssDNA oligos were 5′ radio-labelled with ^{32}P. For 28S 4189 and 28S 4190 (negative and positive controls) probing 10 μg total RNA from HIV-1 infected MT4 cells was used. For A7877 and A7883 1 μg poly(A) RNA from HIV-1 infected MT4 cells was used. RNA and radio-labeled DNA oligos (1 μl) were annealed in 2 × annealing solution in a total volume of 15 μl with 1 × *Tth* pol buffer with 1 mM $MnCl_2$ (Promega) or AMV buffer (Promega), The mixture was denatured at 95 °C for 10 min and slowly annealed cooling to room temperature. 3 μl of annealed solution were mixed with 2 μl of enzyme and heated at 37 °C (AMV Reverse Transcriptase) or 55 °C (Tth DNA Polymerase) for 2 min. dTTP solution (final dTTP concentration: 100 μM) was added and the reactions were incubated for 30 min at 37 °C (AMV) or at 55 °C (Tth). Reactions were resolved on a 20% denaturing polyacrylamide gel and exposed overnight on phosphoimaging screen. SsDNA probe sequences are listed in Supplementary Information Table 3.

Accession numbers.—RNA-Seq data are publicly available at GEO GSE74016.

Supplementary Material

Refer to Web version on PubMed Central for supplementary material.

Acknowledgments

We gratefully acknowledge Steve Head and the staff of the Next Generation Sequencing core facility at the Scripps Research Institute for help with early phase of the project and HT-seq. We thank Jennifer Klabis for her help with preparation of figures, and members of the Rana lab for helpful discussions and advice, especially Drs. Ti-Chun Chao and Kungyen Chang.

REFERENCES

1Sharp PA. The centrality of RNA Cell. 2009; 136:577–580. DOI: 10.1016/j.cell.2009.02.007 [PubMed: 19239877]

2Squires JE. Widespread occurrence of 5-methylcytosine in human coding and non-coding RNA Nucleic Acids Res. 2012; 40:5023–5033. DOI: 10.1093/nar/gks144 [PubMed: 22344696]

3Yi C, Pan T. Cellular dynamics of RNA modification Acc Chem Res. 2011; 44:1380–1388. DOI: 10.1021/ar200057m [PubMed: 21615108]

4Desrosiers RC, Friderici KH, Rottman FM. Characterization of Novikoff hepatoma mRNA methylation and heterogeneity in the methylated 5' terminus Biochemistry. 1975; 14:4367–4374. [PubMed: 169893]

5Perry RP, Kelley DE, Friderici K, Rottman F. The methylated constituents of L cell messenger RNA: evidence for an unusual cluster at the 5' terminus Cell. 1975; 4:387–394. [PubMed: 1168101]

6Schibler U, Kelley DE, Perry RP. Comparison of methylated sequences in messenger RNA and heterogeneous nuclear RNA from mouse L cells J Mol Biol. 1977; 115:695–714. [PubMed: 592376]

7Wei CM, Gershowitz A, Moss B. Methylated nucleotides block 5' terminus of HeLa cell messenger RNA Cell. 1975; 4:379–386. [PubMed: 164293]

8Meyer KD. Comprehensive analysis of mRNA methylation reveals enrichment in 3' UTRs and near stop codons Cell. 2012; 149:1635–1646. DOI: 10.1016/j.cell.2012.05.003 [PubMed: 22608085]

9Dominissini D. Topology of the human and mouse m6A RNA methylomes revealed by m6A-seq Nature. 2012; 485:201–206. DOI: 10.1038/nature11112 [PubMed: 22575960]

10Schwartz S. Perturbation of m6A writers reveals two distinct classes of mRNA methylation at internal and 5' sites Cell Rep. 2014; 8:284–296. DOI: 10.1016/j.celrep.2014.05.048 [PubMed: 24981863]

11Frayling TM. A common variant in the FTO gene is associated with body mass index and predisposes to childhood and adult obesity Science. 2007; 316:889–894. DOI: 10.1126/science.1141634 [PubMed: 17434869]

12Jia G. N6-methyladenosine in nuclear RNA is a major substrate of the obesity-associated FTO Nat Chem Biol. 2011; 7:885–887. DOI: 10.1038/nchembio.687 [PubMed: 22002720]

13Zheng G. ALKBH5 is a mammalian RNA demethylase that impacts RNA metabolism and mouse fertility Mol Cell. 2013; 49:18–29. DOI: 10.1016/j.molcel.2012.10.015 [PubMed: 23177736]

14Bokar JA, Shambaugh ME, Polayes D, Matera AG, Rottman FM. Purification and cDNA cloning of the AdoMet-binding subunit of the human mRNA (N6-adenosine)-methyltransferase RNA. 1997; 3:1233–1247. [PubMed: 9409616]

15Ping XL. Mammalian WTAP is a regulatory subunit of the RNA N6-methyladenosine methyltransferase Cell Res. 2014; 24:177–189. DOI: 10.1038/cr.2014.3 [PubMed: 24407421]

16Liu J. A METTL3-METTL14 complex mediates mammalian nuclear RNA N6-adenosine methylation Nat Chem Biol. 2014; 10:93–95. DOI: 10.1038/nchembio.1432 [PubMed: 24316715]

17Jia G, Fu Y, He C. Reversible RNA adenosine methylation in biological regulation Trends Genet. 2013; 29:108–115. DOI: 10.1016/j.tig.2012.11.003 [PubMed: 23218460]

18Lee M, Kim B, Kim VN. Emerging roles of RNA modification: m(6)A and U-tail Cell. 2014; 158:980–987. DOI: 10.1016/j.cell.2014.08.005 [PubMed: 25171402]

19Wang X. N6-methyladenosine-dependent regulation of messenger RNA stability Nature. 2014; 505:117–120. DOI: 10.1038/nature12730 [PubMed: 24284625]

20Xu C. Structural basis for selective binding of m6A RNA by the YTHDC1 YTH domain Nat Chem Biol. 2014; 10:927–929. DOI: 10.1038/nchembio.1654 [PubMed: 25242552]

21Geula S. Stem cells. m6A mRNA methylation facilitates resolution of naive pluripotency toward differentiation Science. 2015; 347:1002–1006. DOI: 10.1126/science.1261417 [PubMed: 25569111]

22Liu N. N(6)-methyladenosine-dependent RNA structural switches regulate RNA-protein interactions Nature. 2015; 518:560–564. DOI: 10.1038/nature14234 [PubMed: 25719671]

23Zhou J. Dynamic m(6)A mRNA methylation directs translational control of heat shock response Nature. 2015; 526:591–594. DOI: 10.1038/nature15377 [PubMed: 26458103]

24Zhao X. FTO-dependent demethylation of N6-methyladenosine regulates mRNA splicing and is required for adipogenesis Cell Res. 2014; 24:1403–1419. DOI: 10.1038/cr.2014.151 [PubMed: 25412662]

25Fustin JM. RNA-methylation-dependent RNA processing controls the speed of the circadian clock Cell. 2013; 155:793–806. DOI: 10.1016/j.cell.2013.10.026 [PubMed: 24209618]

26Geula S. m6A mRNA methylation facilitates resolution of naive pluripotency toward differentiation Science. 2015

27Batista PJ. A RNA modification controls cell fate transition in mammalian embryonic stem cells Cell Stem Cell. 2014; 15:707–719. DOI: 10.1016/j.stem.2014.09.019 [PubMed: 25456834]

28Wang Y. N6-methyladenosine modification destabilizes developmental regulators in embryonic stem cells Nat Cell Biol. 2014; 16:191–198. DOI: 10.1038/ncb2902 [PubMed: 24394384]

29Kane SE, Beemon K. Precise localization of m6A in Rous sarcoma virus RNA reveals clustering of methylation sites: implications for RNA processing Mol Cell Biol. 1985; 5:2298–2306. [PubMed: 3016525]

30Krug RM, Morgan MA, Shatkin AJ. Influenza viral mRNA contains internal N6-methyladenosine and 5'-terminal 7-methylguanosine in cap structures J Virol. 1976; 20:45–53. [PubMed: 1086370]

31Finkel D, Groner Y. Methylations of adenosine residues (m6A) in pre-mRNA are important for formation of late simian virus 40 mRNAs Virology. 1983; 131:409–425. [PubMed: 6318439]

32Fu L. Simultaneous Quantification of Methylated Cytidine and Adenosine in Cellular and Tissue RNA by Nano-Flow Liquid Chromatography-Tandem Mass Spectrometry Coupled with the Stable Isotope-Dilution Method Anal Chem. 2015; 87:7653–7659. DOI: 10.1021/acs.analchem.5b00951 [PubMed: 26158405]

33Heaphy S. HIV-1 regulator of virion expression (Rev) protein binds to an RNA stem-loop structure located within the Rev response element region Cell. 1990; 60:685–693. [PubMed: 1689218]

34Kjems J, Brown M, Chang DD, Sharp PA. Structural analysis of the interaction between the human immunodeficiency virus Rev protein and the Rev response element Proc Natl Acad Sci U S A. 1991; 88:683–687. [PubMed: 1992459]

35Malim MH. HIV-1 structural gene expression requires binding of the Rev trans-activator to its RNA target sequence Cell. 1990; 60:675–683. [PubMed: 2406030]

36Battiste JL. Alpha helix-RNA major groove recognition in an HIV-1 rev peptide-RRE RNA complex Science. 1996; 273:1547–1551. [PubMed: 8703216]

37Harcourt EM, Ehrenschwender T, Batista PJ, Chang HY, Kool ET. Identification of a selective polymerase enables detection of N(6)-methyladenosine in RNA J Am Chem Soc. 2013; 135:19079–19082. DOI: 10.1021/ja4105792 [PubMed: 24328136]

38Heaphy S, Finch JT, Gait MJ, Karn J, Singh M. Human immunodeficiency virus type 1 regulator of virion expression, rev, forms nucleoprotein filaments after binding to a purine-rich “bubble” located within the rev-responsive region of viral mRNAs Proc Natl Acad Sci U S A. 1991; 88:7366–7370. [PubMed: 1871141]

39Tiley LS, Malim MH, Tewary HK, Stockley PG, Cullen BR. Identification of a high-affinity RNA-binding site for the human immunodeficiency virus type 1 Rev protein Proc Natl Acad Sci U S A. 1992; 89:758–762. [PubMed: 1731351]

40Kjems J, Calnan BJ, Frankel AD, Sharp PA. Specific binding of a basic peptide from HIV-1 Rev EMBO J. 1992; 11:1119–1129. [PubMed: 1547776]

41Hammerschmid M. Scanning mutagenesis of the arginine-rich region of the human immunodeficiency virus type 1 Rev trans activator J Virol. 1994; 68:7329–7335. [PubMed: 7523698]

42Alarcon CR. HNRNPA2B1 Is a Mediator of m(6)A-Dependent Nuclear RNA Processing Events Cell. 2015; 162:1299–1308. DOI: 10.1016/j.cell.2015.08.011 [PubMed: 26321680]

43Roost C. Structure and Thermodynamics of N-Methyladenosine in RNA: A Spring-Loaded Base Modification J Am Chem Soc. 2015

44Spitale RC. Structural imprints in vivo decode RNA regulatory mechanisms Nature. 2015; 519:486–490. DOI: 10.1038/nature14263 [PubMed: 25799993]

45Saletore Y. The birth of the Epitranscriptome: deciphering the function of RNA modifications Genome Biol. 2012; 13:175. [PubMed: 23113984]

46Dobin A. STAR: ultrafast universal RNA-seq aligner Bioinformatics. 2013; 29:15–21. DOI: 10.1093/bioinformatics/bts635 [PubMed: 23104886]

47Quinlan AR, Hall IM. BEDTools: a flexible suite of utilities for comparing genomic features Bioinformatics. 2010; 26:841–842. DOI: 10.1093/bioinformatics/btq033 [PubMed: 20110278]

48Robinson MD, McCarthy DJ, Smyth GK. edgeR: a Bioconductor package for differential expression analysis of digital gene expression data Bioinformatics. 2010; 26:139–140. DOI: 10.1093/bioinformatics/btp616 [PubMed: 19910308]

49Kalland KH, Szilvay AM, Langhoff E, Haukenes G. Subcellular distribution of human immunodeficiency virus type 1 Rev and colocalization of Rev with RNA splicing factors in a speckled pattern in the nucleoplasm J Virol. 1994; 68:1475–1485. [PubMed: 8107211]

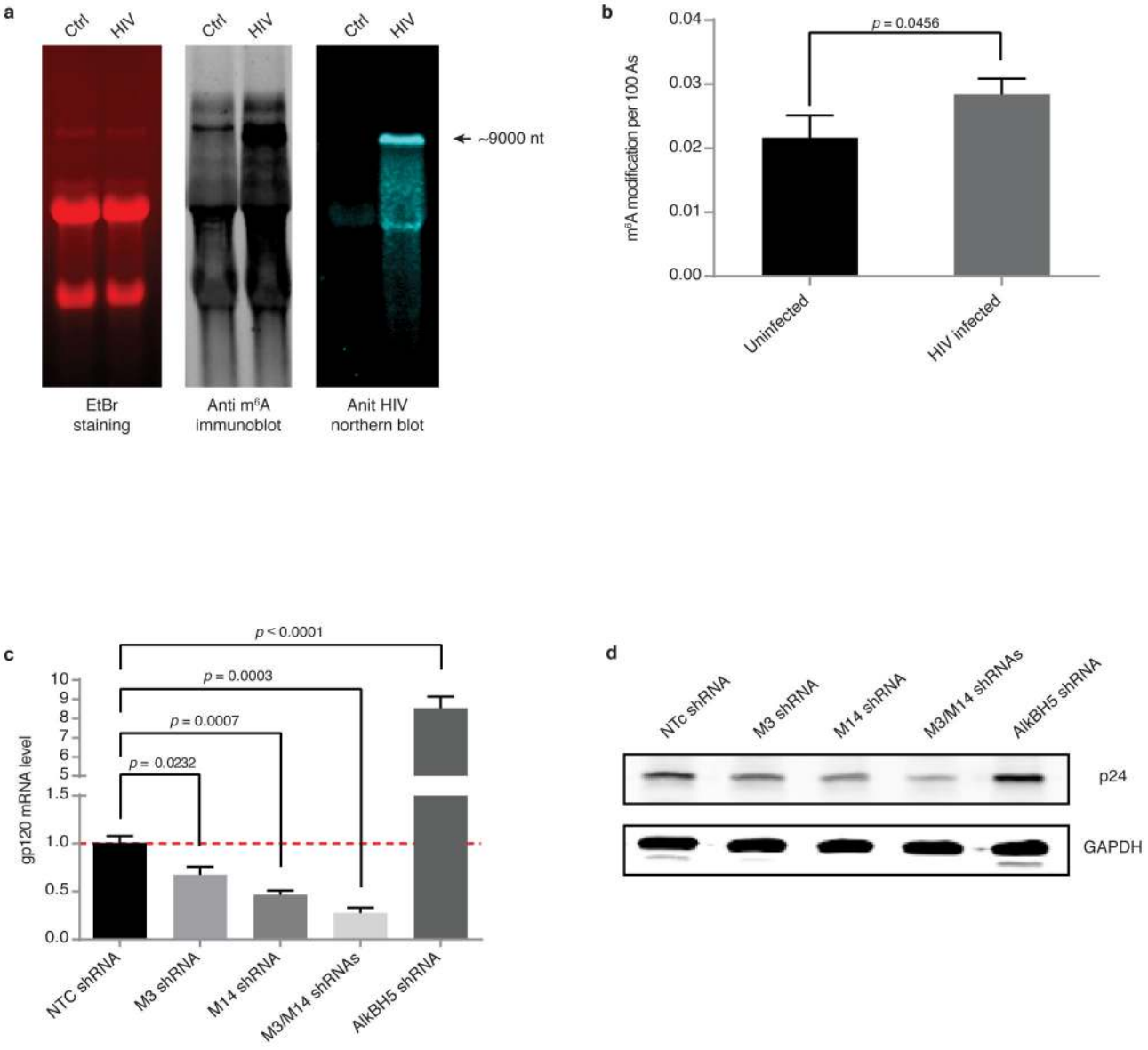

Figure 1. m^{6}A RNA methylation in T cells is promoted by HIV-1 infection and modulates viral replication.

a, Analysis of RNA from HIV-1-infected T cells. Total RNA extracted from uninfected (Ctrl) or HIV-1-infected (HIV) MT4 cells 3 days post-infection was analysed by ethidium bromide (EtBr) staining (left), anti-m^{6}A immunoblotting (middle), or northern blotting for HIV-1 RNA (right). Arrow indicates the predicted size of full-length HIV-1 RNA. The data is a representative of seven independent experiments. **b,** LC-MS/MS quantification of m^{6}A content in poly(A) enriched RNA fractions. Results are the mean ± s.e.m. of five independent experiments. *P* values were calculated by unpaired two-tailed Student's *t*-test. **c, d,** HIV-1 replication is reduced by METTL3 and METTL14 silencing and enhanced by AlkBH5 silencing. **c,** RT-qPCR analysis of gp120 expression in MT4 cells transduced for 3 days with nontargeting control (NTC), METTL3, METTL14, or AlkBH5 shRNA. Cells were then infected with HIV-1 LAI virus, and cells were analysed 3 days later. **d,** Western

blot analysis of HIV-1 p24 intracellular protein expression in cells described in **c**. Results are the mean ± s.e.m. of four independent experiments. *P* values were calculated by unpaired two-tailed Student's *t*-test.

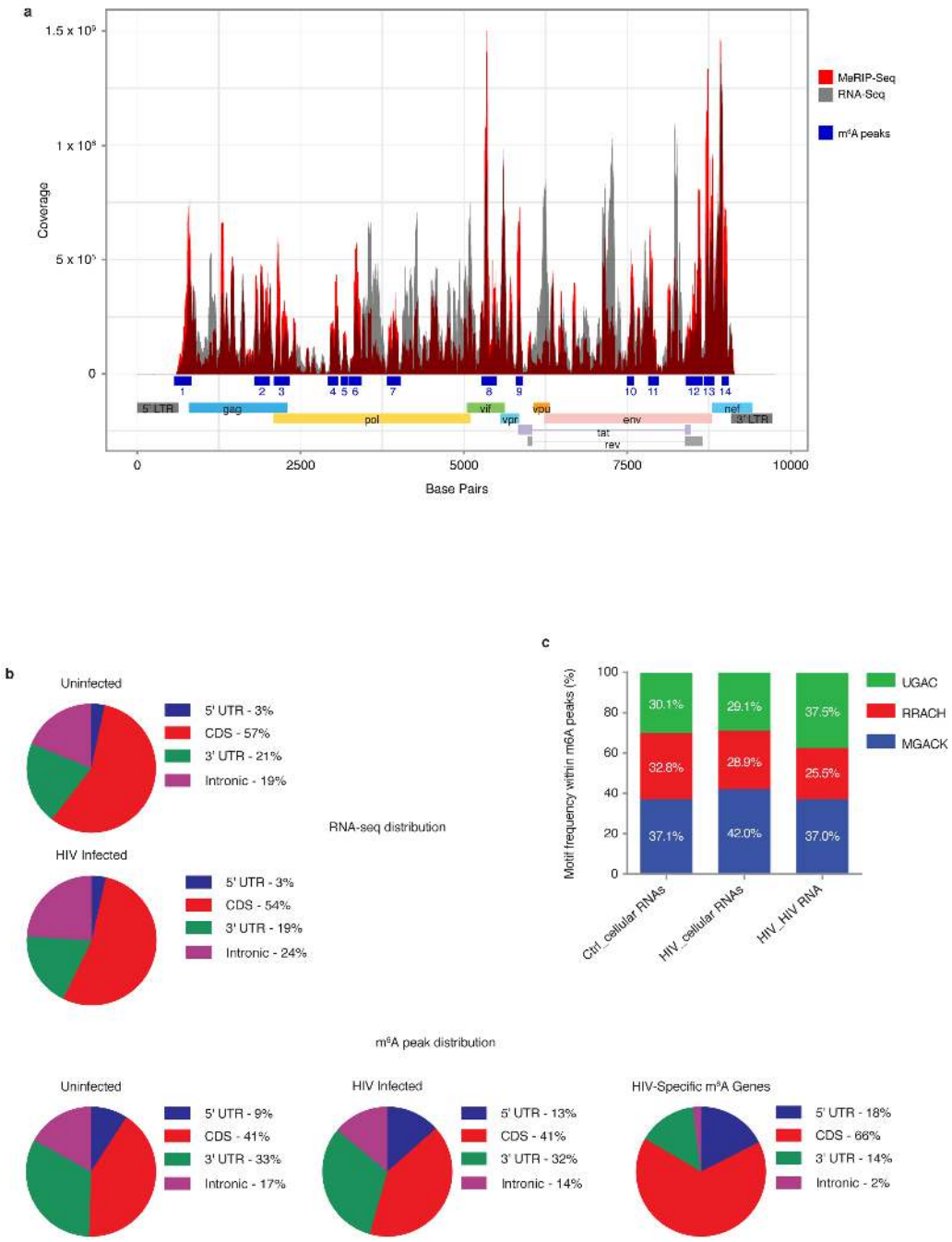

Figure 2. RNA methylation profiles of HIV-1 and HIV-1-infected T cells.

a, Methylation peaks in the full-length HIV-1 RNA genome. Viral gene annotation is shown below. Poly(A) RNA from uninfected and HIV-1-infected MT4 cells was fragmented, subjected to RNA-seq and MeRIP-seq, and analysed as described previously8. The grey shading corresponds to the total RNA-seq mapping distribution (MeRIP input), and the red signal corresponds to the MeRIP-seq mapping distribution. On the x-axis, the dark blue boxes and numbers indicate the m^{6}A peaks called by MeRIPPeR analysis and referred to in the text. **b,** Topology of m^{6}A in the cellular and viral transcriptomes. Pie charts showing the

distribution of total RNA sequence (upper) and m^6A peaks (middle) in four regions (5′UTR, CDS, 3′UTR, and intronic) of transcripts from uninfected and HIV-1-infected MT4 cells. m^6A peak distribution in HIV-1-specific RNA is also shown (bottom). **c,** Frequency of TGAC, RRACH, and MGACK sequence motifs within m^6A peaks in cellular RNAs from control and HIV-1-infected MT4 cells (Ctrl_cellular RNAs and HIV_cellular RNAs, respectively) and HIV-1 LAI RNA (HIV_HIV RNA).

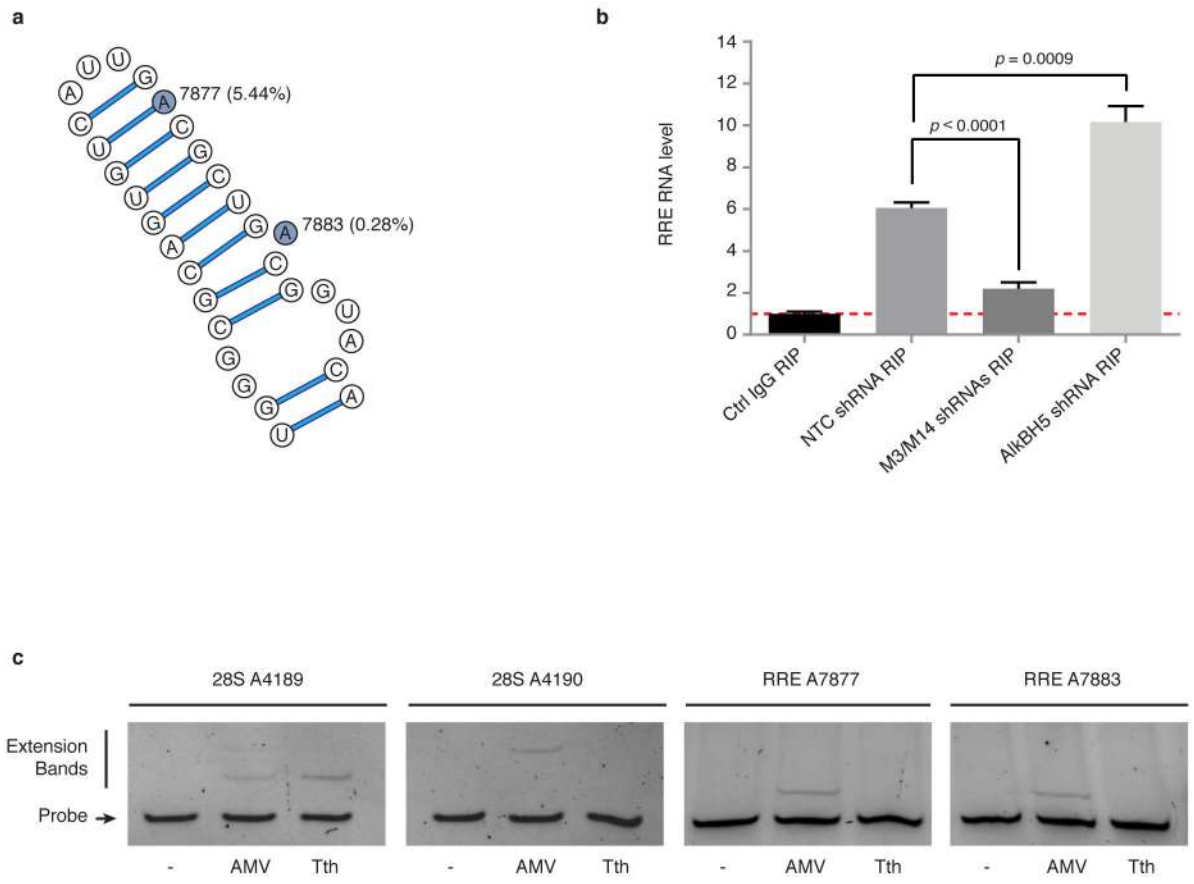

Figure 3. m^{6}A methylation modulates the interaction between Rev protein and RRE RNA.

a, Secondary structure of the hairpin loop IIB of HIV-1 RRE. The two highlighted adenosines represent the methylation sites identified in peak 11 on Figure 2a. Nucleotide numbering is based on the pLAI2 proviral vector sequence, and the mutation frequency of the adenosines in 2,501 HIV-1 sequences is shown in parentheses. **b,** RRE methylation enhances Rev interactions. 293T cells were depleted of METTL3, METTL14, or AlkBH5, and transfected pLAI2 vector. RIP-qPCR experiments were performed by IP with control IgG or anti-Rev antibody followed by qPCR to analyse RRE RNA. Results are the mean ± s.e.m. of 3 independent experiments and are expressed as the fold enrichment of RRE RNA in anti-Rev versus control IgG IPs. *P* values were calculated by unpaired two-tailed Student's *t*-test. **c,** RRE A7877 and A7883 are methylated in vivo. Primers were designed to probe for m^{6}A modification at these two sites in RRE. AMV and *Tth* primer extensions for A7877 and A7883 were performed on 1 μg poly(A) enriched RNA from HIV-1 infected MT4 cells. Extension for 28S A4189 and 28S A4190 were performed on 10 μg total RNA and served as negative and positive methylation sites, respectively.

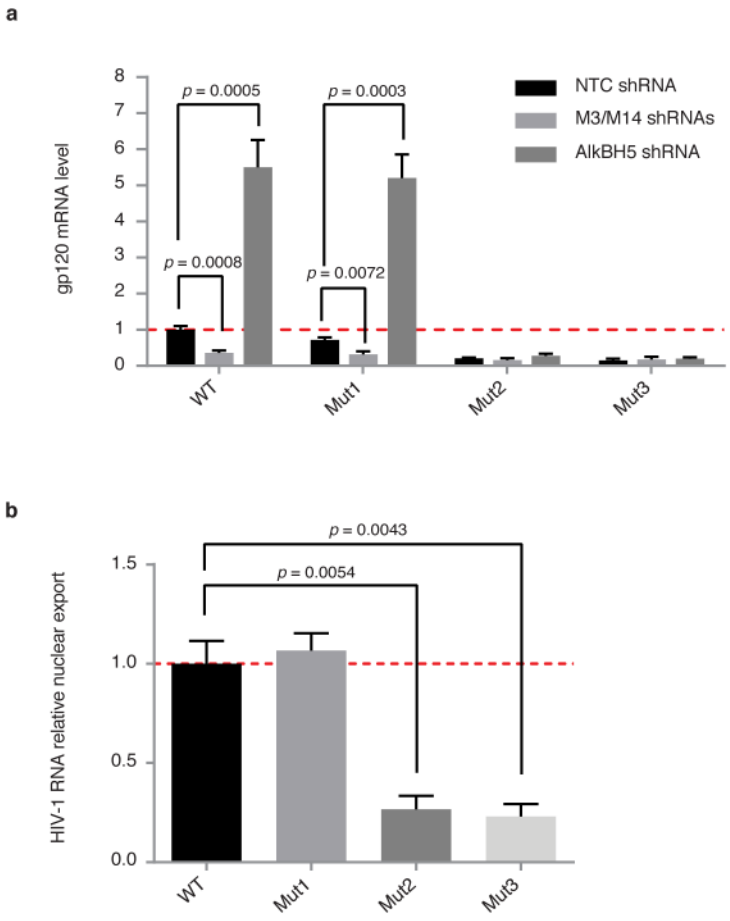

Figure 4. HIV-1 replication and RNA nuclear export are perturbed by methylation of A7883 in the RRE bulge region.

a, WT or LAI HIV-1 mutant constructs, U7871C + A7877G (Mut1), A7883G (Mut2), and the combination of both (Mut3), were assessed for replication in 293T cells under METTL3/METTL14 or AlkBH5 knock-down conditions. Results are the mean ± s.e.m. of three independent experimentsand *P* values were calculated by unpaired two-tailed Student's *t*-test. **b,** Nuclear export of viral RNA was analysed by cytoplasmic and nuclear fractionation in 293T cells transfected with WT or mutant LAI constructs described in **a**. Viral RNA distribution in the two compartments is relative to the viral RNA content from total cellular RNA. Results are the mean ± s.e.m. of three independent experiments. *P* values were calculated by unpaired two-tailed Student's *t*-test.

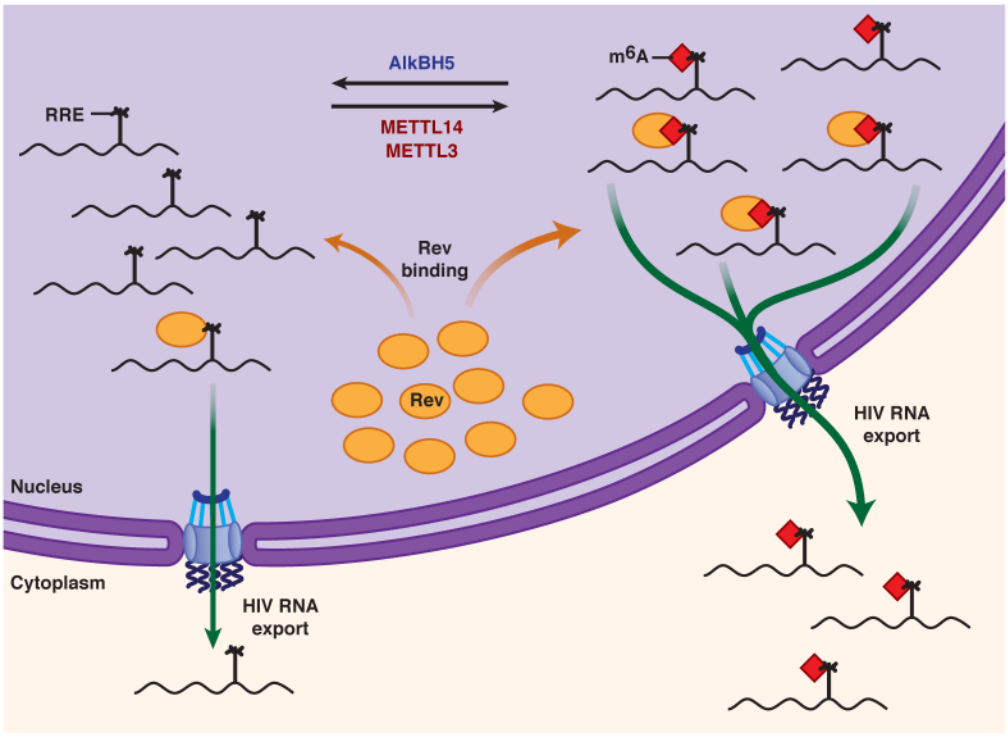

Figure 5.

Proposed model for modulation of the m^{6}A modification in RRE RNA and its effect on HIV-1 replication. See text for details. For simplicity, only monomeric Rev–RRE interactions are shown.

Table 1.

HIV m6A peaks

Peak number	Position (nt)	Features
1	625-875	PBS, DIS, ψ
2	1950-2075	gag CDS
3	2150-2375	gag STOP, pol START
4	3000-3150	pol CDS
5	3175-3275	pol CDS
6	3325-3475	pol CDS
7	3845-4075	pol CDS
8	5325-5450	vif CDS, ESEVpr
9	5850-5950	ESS2p, ESS2, vpr CDS
10	7550-7650	env CDS
11	7875-8000	RRE, env CDS
12	8450-8700	env CDS, rev CDS, tat STOP, ESS3a
13	8725-8875	env CDS, nef START
14	9000-9100	nef CDS

PBS: primary binding site; DIS: dimerization sequence; ψ: encapsidation sequence; CDS: coding sequence; STOP: stop codon; START: start codon; ESE: exonic splicing enhancer; ESS: exonic splicing silencer; RRE: Rev-responsive element.